論文

폭이 변하는 Transversely Isotropic 판의 탄성좌굴

윤순종*+, 정재호**

Elastic Buckling of Transversely Isotropic Plate with Variable Width

S. J. Yoon*+, J. H. Jung**

ABSTRACT

Presented in this paper are the results of an analytical investigation pertaining to the elastic buckling behavior of transversely isotropic plate with variable width subjected to unequal uniaxial compression forces at the ends and in-plane shear forces at the sides. The existing analytical solution developed for the isotropic plates is extended so that the transversely isotropic material properties can be taken into account in the plate buckling analyses. For the derivation of buckling equation the power series solution is employed. Graphical forms of results for finding the buckling strength of tapered plates are presented. In addition, the finite element analysis is also conducted. The results are compared and discussed.

초 록

본 연구는 폭이 변하는 transversely isotropic 판에서 평행한 변에 서로 크기가 다른 면내 축방향 압축력이 작용하며, 경사진면에는 면내 전단력이 작용하는 경우 판의 탄성좌굴거동에 관한 해석적 연구결과이다. 폭이 변하는 등방성판의 좌굴해석을 위해 개발된 기존의 이론적 해를 확장하여 transversely isotropic 재료의 역학적 성질을 고려한 좌굴해석을 할 수 있도록 하였다. 이론식은 power series를 사용하여 유도하였으며, 유한요소해석을 부가적으로 수행하고 그 결과를 이론식을 사용한 해석결과와 비교, 검토하였다.

1. Introduction

During the past two decades, the demand of fiber reinforced plastics (FRP) have been greatly increased not only in new civil engineering construction but also in the retrofitting and strengthening of existing structures. Many international industries are currently producing various shapes of FRP structural profiles with thin-walled component elements. The theoretical and experimental investigations of FRP structural members have been performed and reported to establish the design guidelines or design criteria of FRP structural members.

Composite materials have many attractive characteristics that are different from the conventional engineering materials. The mechanical properties of FRP are common to consider as an anisotropic material. But for the unidirectional fiber reinforced thin-walled structural profiles (such as pultruded structural sections), the material can be assumed to be the transversely isotropic in the classical small-deflection problems.

In this paper, we present the results of an analytical investigation pertaining to the buckling strength of transversely isotropic plate with variable width. In the design of bridges, ships, automobiles, and aircraft structures, problems involving the stability of plate having variable width may arise frequently. Sometimes, for a structure to carry

*+ 홍익대학교 공과대학 토목공학과 부교수, 교신저자(E-mail:sjyoon@wow.hongik.ac.kr)
** 홍익대학교 대학원 토목공학과 박사과정

variable compressive forces more efficiently, it may be necessary to alter its thickness and/or width. Therefore, the knowledge of critical load of non-rectangular plate is desirable.

In this paper, the buckling problem of transversely isotropic plate with variable width is solved by employing the power series solution. The boundary conditions at the parallel edges are assumed to be simply supported and the boundary conditions of sides are both simple and/or fixed. The results are compared with the results obtained by the finite element method.

2. Theoretical Derivations

Rigorous solutions of plate problems are usually limited to a few cases. The problem considered in this paper is one of the difficult problems to find suitable functions by the biharmonic equation for deflection. In this paper, we solved the elastic buckling problem of transversely isotropic tapered plate by using the power series solution. The method adopted in this study was originally developed by Pope [1] for the isotropic tapered plate.

2.1 Basic Assumptions

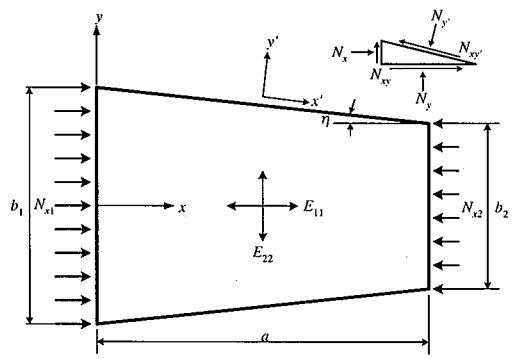

Fig. 1 Transversely isotropic tapered plate.

Fig. 1 shows the transversely isotropic tapered plate. For the sake of simplicity, we assumed that the plate is isosceles trapezoidal, symmetric with respect to x-axis, and the parallel edges are simply supported.

In this figure, E_{11} and E_{22} are the moduli of elasticity in the direction of x-axis and y-axis, respectively. N_{x1} and N_{x2} are uniform normal loads along the parallel ends $x=0$ and $x=a$. a is the length of plate, and $b_i(i=1, 2)$ are widths of each end. η is the angle of inclination at both sides.

In addition to the basic assumptions for the orthotropic plate [2], following assumptions are adopted [1].

(1) Equilibrium is maintained by shear flows along the sides.
(2) Transverse buckled shape is the same as that across a rectangular plate of constant thickness under uniform end load with the same boundary conditions along the sides.
(3) Middle surface force N_x normal to the cross section of x-axis vary linearly along the x-axis of plate with a consistent N_{xy} distribution.

2.2 Middle Surface Forces

In accordance with the assumption (3), the middle surface force N_x can be expressed as:

$$N_x = N_{x1}(\alpha_0 + \alpha_1 X) \tag{1}$$

The most general system of middle surface forces can be made up of Eq. (1), and, N_y and N_{xy} can be derived under the prescribed force boundary conditions on the sides of the plate as shown in Eqs. (2) and (3).

$$N_y = N_{x1}(\beta_0 + \beta_1 X) \tag{2}$$

$$N_{xy} = N_{x1}\gamma Y \tag{3}$$

In Eqs. (1), (2), and (3), all undefined variables are given in Appendix.

The middle surface force N_{x1}, when the buckling occurs, can be defined by Eq. (4) following Timoshenko (1961)[3] by introducing k_1 the plate buckling coefficient.

$$N_{x1} = k_1 \frac{\pi^2 \sqrt{D_{11} D_{22}}}{b_1^2} \tag{4}$$

In Eq. (4), D_{11} and D_{22} are the flexural rigidities in 1-1 and 2-2 material property directions, and those are defined as follows:

$$D_{11} = \frac{E_{11} t^3}{12(1-\nu_{12}\nu_{21})} \tag{5a}$$

$$D_{22} = \frac{E_{22} t^3}{12(1-\nu_{12}\nu_{21})} \tag{5b}$$

In Eqs. (5 a, b), t is the thickness of plate, and ν_{12} and ν_{21} are the Poisson's ratios in the direction of major and minor axis, respectively.

2.3 Buckling Equation

In the classical small-deflection theory, the increment of the total potential energy of transversely isotropic plate due to the infinitesimal arbitrary variation δw of the deflection must be vanished. This condition is given by:

$$\int\int \delta w\Big\{D_{11}\frac{\partial^4 w}{\partial x^4}+2H\frac{\partial^4 w}{\partial x^2\partial y^2} + D_{22}\frac{\partial^4 w}{\partial y^4}+N_x\frac{\partial^2 w}{\partial x^2} + N_y\frac{\partial^2 w}{\partial y^2}+2N_{xy}\frac{\partial^2 w}{\partial x^2\partial y^2}\Big\}dxdy=0 \tag{6}$$

The deflection function of the plate shown in Fig. 1 can be represented approximately in the non-dimensional form [1]:

$$W=\frac{w}{a}=f(X)\cdot\Phi(\theta) \tag{7}$$

where

$$X=1+\rho\frac{x}{a},\quad \theta=\frac{Y}{X},\quad Y=\frac{y}{b_1},\quad \rho=\frac{b_2}{b_1}-1$$

In Eq. (7), the function $\Phi(\theta)$ represents an assumed deflected shape normal to the x-axis and the function $f(X)$ can be found by the energy method.

Eq. (6) may be expressed in the non-dimensional form by using Eqs. (1), (2), (3), (4), and (7) as shown in Eq. (8).

$$\int\int \delta W\Big\{D_{11}\rho^4\frac{\partial^4 W}{\partial X^4}+2H\rho^2\phi^2\frac{\partial^4 W}{\partial X^2\partial Y^2} + D_{22}\phi^4\frac{\partial^4 W}{\partial Y^4}\Big\}dXdY + \int\int \delta W\Big\{k_1\pi^2\sqrt{D_{11}D_{22}}\Big(\rho^2 k_x\frac{\partial^2 W}{\partial X^2} + \phi^2 k_y\frac{\partial^2 W}{\partial Y^2} + 2\rho\phi\gamma Y\frac{\partial^2 W}{\partial X\partial Y}\Big)\Big\}dXdY=0 \tag{8}$$

In Eq. (8), H, ϕ, k_x, and k_y are also given in Appendix.

Since Φ is an assumed function in expression for the deflection W, δW can be expressed:

$$\delta W=\Phi\cdot\delta f \tag{9}$$

Because the variation δf is arbitrary, the integration with respect to X can be removed from Eq. (8). Substituting Eq. (7) into the ensuing equation and integrating with respect to Y, the following differential equation is obtained for f.

$$\begin{aligned} &p_4X^4\frac{d^4f}{dX^4}+p_3X^3\frac{d^3f}{dX^3}\\ &+(p_2+q_2X^2+r_2X^3)X^2\frac{d^2f}{dX^2}\\ &+(p_1+q_1X^2+r_1X^3)X\frac{df}{dX}\\ &+(p_0+q_0X^2+r_0X^3)f=0 \end{aligned} \tag{10}$$

Eq. (10) can be solved by expanding f as a power series as shown in Eq. (11). The function f can be expressed in terms of Z, which is introduced to improve the convergence of the series at the ends of the plate at $X=1$ and $X=1+\rho$.

$$f=\sum_{n=0}^{\infty}a_nZ^n \tag{11}$$

where

$$Z=X-\lambda,\quad \lambda=1+0.5\rho$$

Upon differentiating Eq. (11) and substituting the appropriate terms into Eq. (10), one can show, without difficulty, that all coefficients a_{n+4} can be obtained by recurrence relations in terms of a_0, a_1, a_2, and a_3, and then Eq. (11) can be written in the form:

$$\begin{aligned} f=&\Big\{1+\sum_{n=0}^{\infty}B_{0n}Z^{n+4}\Big\}a_0\\ &+\Big\{Z+\sum_{n=0}^{\infty}B_{1n}Z^{n+4}\Big\}a_1\\ &+\Big\{Z^2+\sum_{n=0}^{\infty}B_{2n}Z^{n+4}\Big\}a_2\\ &+\Big\{Z^3+\sum_{n=0}^{\infty}B_{3n}Z^{n+4}\Big\}a_3 \end{aligned} \tag{12}$$

In Eq. (12), the B_{in} (n=1, 2, ···) with $i=0, 1, 2$, and 3, are defined as follows:

$$B_{in}=-\frac{1}{C_8(n)}\Big\{C_{m_i}(n)+\sum_{j=0}^{n-1}C_j(n)B_{ij}\Big\} \tag{13}$$

In Eq. (13), $C_j(n)$ (j=1, 2, ···, 8) are given in Appendix, and B_{i0}, m_i, and l are as follow:

$$B_{00}=-\frac{C_4(0)}{C_8(0)},\quad B_{10}=-\frac{C_5(0)}{C_8(0)}$$

$$B_{20}=-\frac{C_6(0)}{C_8(0)},\quad B_{30}=-\frac{C_7(0)}{C_8(0)}$$

$$m_i=4+i-n\geq 1,\quad l=8-(n-j)\geq 1$$

Four linear simultaneous equations are obtained for the constants a_i (i=0, 1, 2, 3) from the boundary conditions along the ends. Since the ensuing simultaneous linear equations are homogeneous, the determinant of coefficient of a_i must be vanished to get the solution other than the trivial one. Using the numerical analysis technique such as the secant method, the buckling coefficient of plate k_1 at wide width with a certain value of plate aspect ratio ϕ, angle of sides η, and ratio of axial load N_{x2}/N_{x1}.

3. Buckling of Transversely Isotropic Plate with Variable Width

3.1 Plate Simply Supported Along the Sides

In accordance with assumption (2), we assume the buckled form along the transverse direction:

$$\Phi(\theta)=\cos\pi\theta \tag{14}$$

The deflection function consisted with Eqs. (12) and (14) satisfy the condition of deflection but does not completely satisfy the condition of moment for simple support along the sides of the plate. However, in previous work by Pope (1962)[1] for the isotropic plate with the same geometric conditions, it was verified that the total work done on the plate by the spurious moments introduced along the sides was zero.

Adopting the boundary conditions ($W=0$, $M_x=0$) at $X=1$ and $X=1+\rho$, the linear homogeneous simultaneous equations can be formed and upon setting the determinant of the coefficient matrix to zero, the characteristic equation can be derived.

Using the numerical analysis technique, the buckling coefficient of transversely isotropic plate k_1 at the wide width of plate with respect to length and wide width ratio a/b_1 can be obtained, and the results are represented in a graphical form as shown in Fig. 2 when N_{x2}/N_{x1} are 0.8 and 1.0, respectively.

In order to verify the ensuing equation the transversely isotropic material properties are replaced with isotropic ones, and the results are plotted in Fig. 3. the results obtained coincide with published ones [1].

3.2 Plate Fixed Along the Sides

In this case, the deflection function along the transverse direction can be assumed as:

$$\Phi(\theta)=\cosh p\theta-q\cos p\theta \tag{15}$$

In Eq. (16), p is the first positive root (4.73004) of the Eq. (16), and q is defined in Eq. (17).

$$\sinh\frac{p}{2}\cos\frac{p}{2}+\cosh\frac{p}{2}\sin\frac{p}{2}=0 \tag{16}$$

$$q=\frac{\cosh\frac{p}{2}}{\cos\frac{p}{2}} \tag{17}$$

The deflection function in Eq. (15) satisfies completely the boundary conditions along the sides.

Adopting the boundary conditions ($W=0$, $M_x=0$) at $X=1$ and $X=1+\rho$, the linear homogeneous simultaneous equations can be formed and upon setting the determinant of the coefficient matrix to zero, the characteristic equation can be derived.

Using a method similar to the case of simply supported sides of plate, the buckling coefficient k_1 with respect to a/b_1 is plotted for a series of values b_2/b_1 when $N_{x2}/N_{x1}=0.8$ and 1.0. To verify the accuracy of results, transversely isotropic material properties were replaced with isotropic ones. Identical results given in Pope (1962)[1] are obtained. The graphical form of results is shown in Fig. 4 for transversely isotropic plates and Fig. 5 for isotropic plates, respectively.

4. Finite Element Analysis

For the finite element analysis, the commercial structural analysis program GTSTRUDL (version 2001)[5] is used. The GTSTRUDL elements used in the modeling of tapered plate are SBHQ6 (Stretching Bending Hybrid Quadrilateral) and

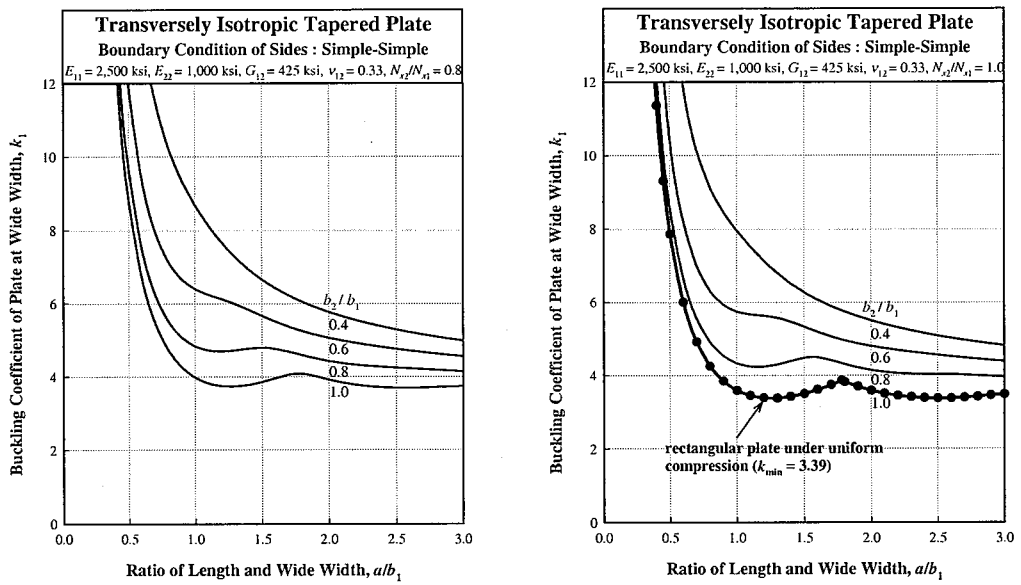

(a) $N_{x2}/N_{x1} = 0.8$ (b) $N_{x2}/N_{x1} = 1.0$

Fig. 2 Buckling coefficient of transversely isotropic tapered plate: simply supported at sides [4].

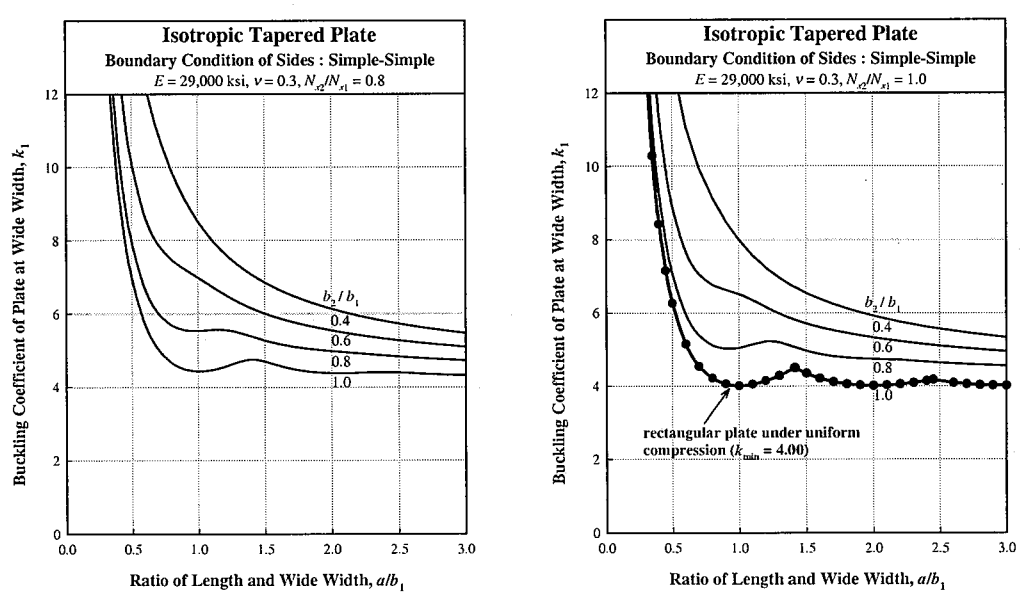

(a) $N_{x2}/N_{x1} = 0.8$ (b) $N_{x2}/N_{x1} = 1.0$

Fig. 3 Buckling coefficient of isotropic tapered plate: simply supported at sides.

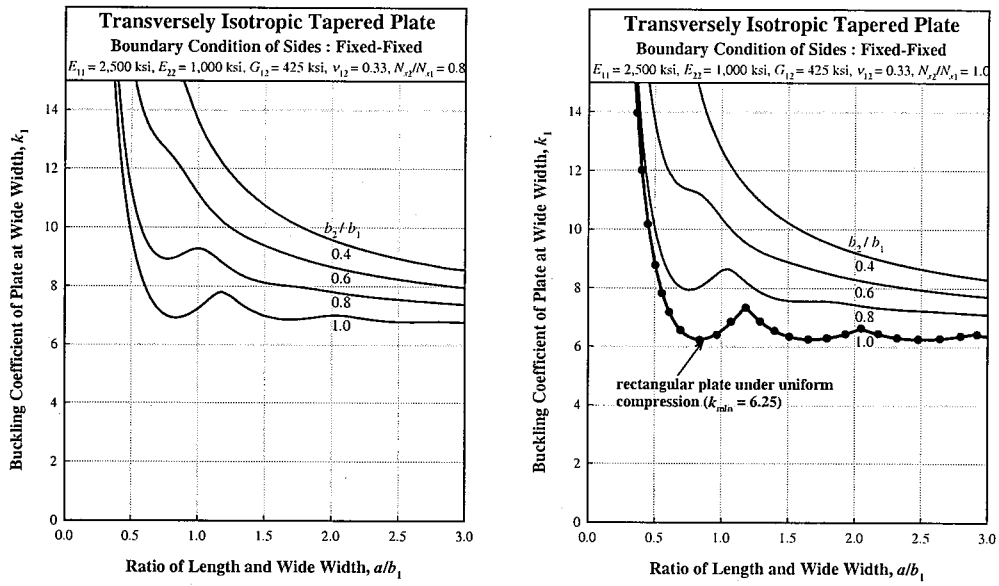

(a) $N_{x2}/N_{x1} = 0.8$ (b) $N_{x2}/N_{x1} = 1.0$

Fig. 4 Buckling coefficient of transversely isotropic tapered plate: fixedly supported at sides (Strongwell, 1997)[4].

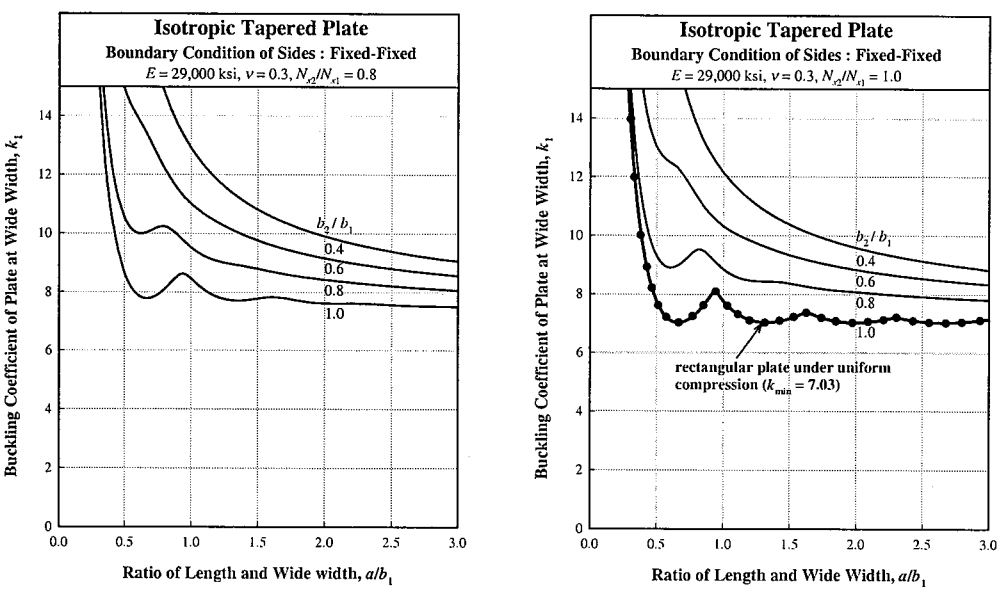

(a) $N_{x2}/N_{x1} = 0.8$ (b) $N_{x2}/N_{x1} = 1.0$

Fig. 5 Buckling coefficient of isotropic tapered plate: fixedly supported at sides.

SBHT6 (Stretching Bending Hybrid Triangular) elements, which are combination of the plane stress and plate bending element. Fig. 6 shows the elements and the degree of freedom (DOF) at node 3.

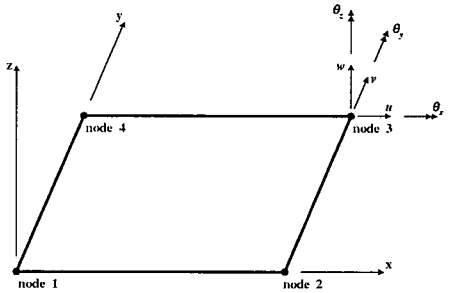

(a) SBHQ6 plate element with DOF at node 3

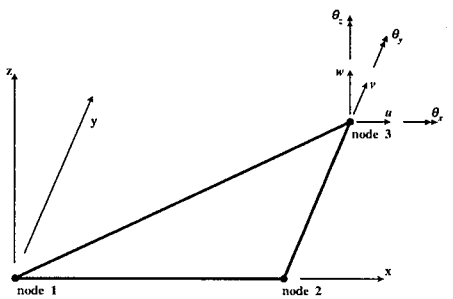

(b) SBHT6 plate element with DOF at node 3

Fig. 6 SBHQ6 and SBHT6 elements.

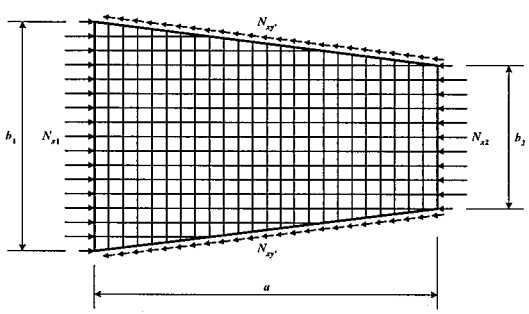

Fig. 7 Model of tapered plate.

Fig. 7 shows the modeling and loading condition of isosceles trapezoidal plate. The unit nodal forces are applied at wide width and 0.2 to 1.0 uniform nodal forces are applied at narrow width. According to the assumption (1), the uniform shear forces are applied at the sides to adjust the state of force equilibrium.

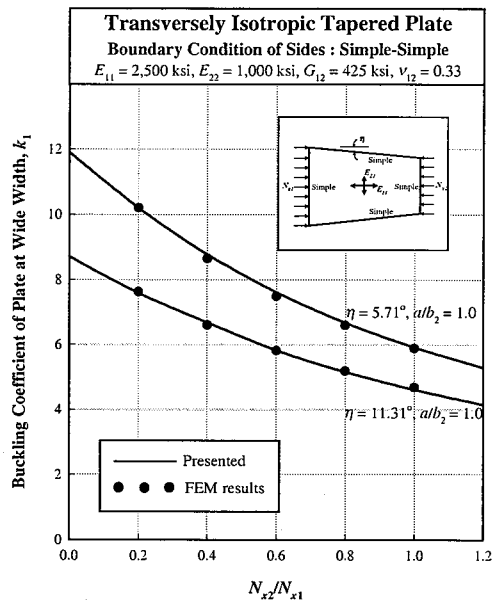

Fig. 8 Comparison of results (simply supported at the sides).

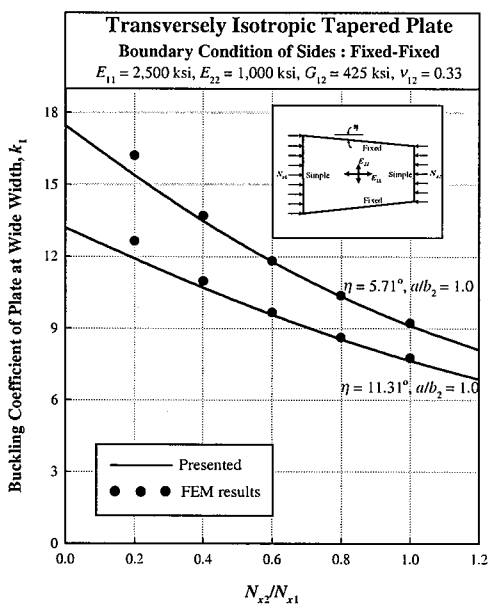

Fig. 9 Comparison of results (fixedly supported at the sides).

Results obtained by using derived equation are compared with the results of finite element analysis. Figs. 8 and 9 show the buckling coefficient k_1 when $\eta = 5.71^o$ and $\eta = 11.31^o$ at a/b_2 = 1.0.

5. Discussion and Conclusions

In this paper, the results of elastic buckling analysis for a transversely isotropic tapered plate subjected to non-equal uniaxial compression forces at the ends and shear forces at the sides are presented.

The equations derived in this study were verified by replacing isotropic material properties instead of transversely isotropic ones and the ensuing equations were compared with existing equations which were derived for a tapered plate with isotropic material. Identical results given in Pope (1962) were obtained.

The buckling analysis of rectangular plate subjected to uniform in-plane compressive forces were also conducted by using the derived equations, and the results (bold line with circled symbol in Fig. 2(b), 3(b), 4(b), and 5(b)) also coincided with published ones [6, 7].

As a matter of course, increasing a/b_2 and/or b_2/b_1, the angle of sloped sides was converge to zero, then the plate changed to rectangular shape. In results, the buckling coefficient of tapered plate converged to that of the rectangular plate.

Finite element analyses were also conducted and the results were compared with theoretical ones obtained by the derived equations. The differences between results of both methods were less than 2 % when N_{x2}/N_{x1} was greater than 0.4. But when N_{x2}/N_{x1} was less than 0.4, the difference was increased (maximum 6 %). The differences of results were also decreased as increasing the a/b_2 and/or b_2/b_1.

These trends of differences between results may be caused by assuming the deflected shape in the transverse direction of the plate as that of the rectangular plate with same boundary condition under uniform compression. Therefore further study needs to be performed to find the proper expression of the deflection function in the transverse direction of tapered plate when the angle of sloped sides becomes large.

Acknowledgement

This research was supported by the 2001 Hongik University Academic Research Support Fund.

Reference

1) Pope, G. G., "The Buckling of Plates Tapered in Planform," *A.R.C. Reports and Memoranda* 3324, April, 1962.
2) Lekhnitskii, S. G., *Anisotropic Plates*, S. W. Tsai and T. Cheron (Trans.), Gordon and Breach, 2nd printing, New York, 1984.
3) Timoshenko, S. P. and Gere, J. M., *Theory of Elastic Stability*, 2nd ed., McGraw-Hill, New York, 1961.
4) Strongwell, *Extern Fiberglass Structural Shapes Design Manual*, Morrison Molded Fiberglass Company, Bristol, Virginia, 1998.
5) GTSTRUDL, *GTSTRUDL User's Manual*, Latest Revision, K, May, GTICS Systems Laboratory, Georgia Institute of Technology, Atlanta, Georgia, 2001.
6) Bulson, P. S., "Local Instability Problems of Light Alloy Struts," *The Aluminium Development Association, Research Report*, No. 29, London, 1955.
7) Yoon, S. J., "Local Buckling of Pultruded I-Shape Column s," *Ph.D. Thesis*, School of Civil Engineering, Georgia Institute of Technology, Atlanta, Georgia, 1993.

Appendix

$$\alpha_0=1-\frac{\Delta}{\rho},\quad \alpha_1=\frac{\Delta}{\rho},\quad \beta_0=-\frac{\rho^2}{4\phi^2}\alpha_0,\quad \beta_0=-\frac{3\rho\Delta}{4\phi^2},\quad \gamma=-\frac{\Delta}{\phi}$$

$$\phi=\frac{a}{b_1},\quad \Delta=\frac{N_{x2}}{N_{x1}}-1$$

$$H=D_{12}+2D_{66},\quad D_{12}=\nu_{21}D_{11}=\nu_{12}D_{22}$$

$$D_{66}=\frac{G_{12}t^3}{12},\quad h=\nu_{12}\sqrt{\frac{E_{22}}{E_{11}}}+\frac{2(1-\nu_{12}\nu_{21})G_{12}}{\sqrt{E_{11}E_{22}}}$$

$$k_x=\alpha_0+\alpha_1 X,\quad k_y=\beta_0+\beta_1 X$$

$$p_0=(24l_1+36l_2+12l_3+l_4)\rho^4\sqrt{\frac{E_{11}}{E_{22}}}+2h\rho^2\phi^2(6s_0+6s_1+s_2)+m_0\phi^4\sqrt{\frac{E_{22}}{E_{11}}}$$

$$p_1=-4\rho^4(6l_1+6l_2+l_3)\sqrt{\frac{E_{11}}{E_{22}}}-4h\rho^2\phi^2(2s_0+s_1)$$

$$p_2=6\rho^4(l_2+2l_1)\sqrt{\frac{E_{11}}{E_{22}}}+2h\rho^2\phi^2 s_0$$

$$p_3=-4\rho^4 l_1\sqrt{\frac{E_{11}}{E_{22}}},\quad p_4=\rho^4 l_0\sqrt{\frac{E_{11}}{E_{22}}}$$

$$q_0=k_1\pi^2\{\rho^2\alpha_0(l_2+2l_1)+\phi^2\beta_0 s_0\}$$

$$q_1=-2k_1\pi^2\rho^2 l_1\alpha_0$$

$$q_2=k_1\pi^2\rho^2 l_0\alpha_0$$

$$r_0=k_1\pi^2\{\rho^2\alpha_1(l_2+2l_1)+\phi^2\beta_1 s_0-2\rho\phi\gamma(l_1+l_2)\}$$

$$r_1=-2k_1\pi^2\rho l_1(\rho\alpha_1-\mu\gamma)$$

$$r_2=k_1\pi^2\rho^2 l_0\alpha_1$$

$$l_0=\int_{-0.5}^{0.5}\Phi^2 d\theta,\quad l_i=\int_{-0.5}^{0.5}\theta^i\Phi\frac{d^i\Phi}{d\theta^i}\,d\theta$$

$$s_i=\int_{-0.5}^{0.5}\theta^i\Phi\frac{d^{i+2}\Phi}{d\theta^{i+2}}\,d\theta,\quad m_0=\int_{-0.5}^{0.5}\Phi\frac{d^4\Phi}{d\theta^4}\,d\theta$$

$$C_1(n)=r_0+(n-3)r_1+(n-3)(n-4)r_2$$

$$\begin{aligned}C_2(n)&=q_0+3r_0\lambda+(n-2)(q_1+4r_1\lambda)\\&\quad+(n-2)(n-3)(q_2+5r_2\lambda)\end{aligned}$$

$$\begin{aligned}C_3(n)&=\lambda\{2q_0+3r_0\lambda+(n-1)(3q_1+6r_1\lambda)\\&\quad+(n-1)(n-2)(4q_2+10r_2\lambda)\}\end{aligned}$$

$$\begin{aligned}C_4(n)&=p_0+q_0\lambda^2+r_0\lambda^3+n(p_1+3q_1\lambda^2+4r_1\lambda^3)\\&\quad+n(n-1)(p_2+6q_2\lambda^2+10r_2\lambda^3)\\&\quad+n(n-1)(n-2)\{p_3+(n-3)p_4\}\end{aligned}$$

$$\begin{aligned}C_5(n)&=\lambda(n+1)\{p_1+q_1\lambda^2+r_1\lambda^3\\&\quad+n(2p_2+3q_2\lambda^2+5r_2\lambda^3)\\&\quad+4n(n-1)(n-2)p_4\}\end{aligned}$$

$$\begin{aligned}C_6(n)\ n&=\lambda^2(n+1)(n+2)\{p_2+q_2\lambda^2+r_2\lambda^3\\&\quad+3np_3+6n(n-1)p_4\}\end{aligned}$$

$$C_7(n)=\lambda^3(n+1)(n+2)(n+3)(p_3+4np_4)$$

$$C_8(n)=\lambda^4(n+1)(n+2)(n+3)(n+4)p_4$$

Unit Conversion

1 ksi = 1 kip/in^2 = 6.89 MPa = 70.31 kgf/cm^2
1 kip = 1,000 lb = 4.45 kN = 453.6 kgf
1 in = 2.54 cm